binary systems in the near-Earth, main-belt, and Kuiper-belt populations, because they provide a wealth of information about physical properties, formation processes, and collisional environments (*38*–*40*).
8. Kalliope was named for the Muse of heroic poetry (*41*). The authors propose that the companion be named Linus, who in various Greek mythological accounts is portrayed as the son of Kalliope and the inventor of melody and rhythm.
9. P. L. Wizinowich *et al.*, *Proc. SPIE* **4007**, 2 (2000).
10. I. S. McLean *et al.*, *Proc. SPIE* **3354**, 566 (1998).
11. T. L. Hayward *et al.*, *Publ. Astron. Soc. Pac.* **113**, 105 (2001).
12. J. L. Margot *et al.*, *Science* **296**, 1445 (2002).
13. The software has been thoroughly validated with a wide range of binary systems, including near-Earth and main-belt asteroids, the Pluto-Charon system (*42*), the 1998 WW31 KBO binary (*43*), and binary stars (*44*).
14. E. F. Tedesco, P. V. Noah, M. Noah, S. D. Price, *Astron. J.* **123**, 1056 (2002).
15. P. Magnusson *et al.*, *Asteroids, Comets, Meteors 1993* (1994), pp. 471–476.
16. P. Magnusson, *Icarus* **85**, 229 (1990).
17. C. D. Murray, S. F. Dermott, *Solar System Dynamics* (Cambridge Univ. Press, 1999).
18. The time scales for orbital plane precession due to the influence of the Sun and Jupiter are on the order of 2500 years and can be neglected.
19. R. Greenberg, *Astron. J.* **86**, 912 (1981).
20. C.-I. Lagerkvist, A. Claesson, *Earth Moon Planets* **72**, 219 (1996).
21. This is unlike some binary Kuiper belt objects that have so much angular momentum that formation by breakup of a single body is not conceivable (*38*). The amount of orbital angular momentum in the Kalliope system is not sufficient to invoke formation by spin-up of the primary beyond the breakup rate and mass shedding, as in the case of near-Earth asteroid binaries (*12*).
22. P. Goldreich, S. Soter, *Icarus* **5**, 375 (1966).
23. A. M. Dziewonski, D. L. Anderson, *Phys. Earth Planet. Int.* **25**, 297 (1981).
24. P. Goldreich, *Mon. Not. R. Astron. Soc.* **126**, 257 (1963).
25. H. He, T. J. Ahrens, *Int. J. Rock Mech. Min. Sci. Geomech.* **31**, 525 (1994).
26. W. M. Kaula, *Rev. Geophys.* **2**, 661 (1964).
27. Using data from a 1937 encounter between 16 Psyche and 94 Aurora, Viateau (*45*) finds that M-type Psyche also has a low density, although the author indicates that there may be biases in the mass determination.
28. D. T. Britt, D. Yeomans, K. Housen, G. Consolmagno, *Asteroids III*, W. F. Bottke, A. Cellino, P. Paolicchi, R. Binzel, Eds. (Univ. of Arizona Press, Tucson, AZ, 2002), pp. 485–500.
29. D. K. Yeomans *et al.*, *Science* **278**, 2106 (1997).
30. J. L. Hilton, *Asteroids III*, W. F. Bottke, A. Cellino, P. Paolicchi, R. Binzel, Eds. (Univ. of Arizona Press, Tucson, AZ, 2002), pp. 103–112.
31. There are independent measurements of the size of Kalliope. E. Bowell, T. Gehrels, and B. Zellner (*46*) obtain a diameter of 175 km with the highest quality code, which gives a density that is 10% higher than the result based on the IRAS value, and a porosity of 65% if one assumes a metallic composition.
32. A. S. Rivkin, E. S. Howell, L. A. Lebofsky, B. E. Clark, D. T. Britt, *Icarus* **145**, 351 (2000).
33. P. S. Hardersen, M. J. Gaffey, P. A. Abell, *Lunar Planet. Inst. Conf. Abstr.* **33**, 1148 (2002).
34. M. J. Gaffey, E. A. Cloutis, M. S. Kelley, K. L. Reed, *Asteroids III*, W. F. Bottke, A. Cellino, P. Paolicchi, R. Binzel, Eds. (Univ. of Arizona Press, Tucson, AZ, 2002), pp. 183–204.
35. S. J. Ostro *et al.*, *Science* **252**, 1399 (1991).
36. C. Magri, G. J. Consolmagno, S. J. Ostro, L. A. M. Benner, B. R. Beeney, *Meteorit. Planet. Sci.* **36**, 1697 (2001).
37. C. Magri, M. C. Nolan, personal communication.
38. J. L. Margot, *Nature* **416**, 694 (2002).
39. J. A. Burns, *Science* **297**, 942 (2002).
40. W. J. Merline *et al.*, *Asteroids III*, W. F. Bottke, A. Cellino, P. Paolicchi, R. Binzel, Eds. (Univ. of Arizona Press, Tucson, AZ, 2002), pp. 289–312.
41. L. D. Schmadel, *Dictionary of Minor Planet Names* (Springer, Berlin, ed. 4, 1999).
42. D. J. Tholen, M. W. Buie, *Icarus* **125**, 245 (1997).
43. C. Veillet *et al.*, *Nature* **416**, 711 (2002).
44. W. D. Heintz, *Astrophys. J. Suppl.* **117**, 587 (1998).
45. B. Viateau, *Astron. Astrophys.* **354**, 725 (2000).
46. E. Bowell, T. Gehrels, B. Zellner, *Asteroids*, T. Gehrels, Ed. (Univ. of Arizona Press, Tucson, AZ, 1979), pp. 1108–1129.
47. We are grateful to M. Britton for follow-up observations at Palomar and to P. Goldreich, T. Ahrens, and M. Pritchard for insightful discussions. J.L.M. thanks S. Kulkarni for financial support. Some of the data presented here were obtained at the W. M. Keck Observatory, which is operated as a scientific partnership among the California Institute of Technology, the University of California, and the National Aeronautics and Space Administration. The observatory was made possible by the generous financial support of the W. M. Keck Foundation. We extend special thanks to those of Hawaiian ancestry on whose sacred mountain we are privileged to be guests. Without their generous hospitality, many of the observations presented here would not have been possible.

17 April 2003; accepted 19 May 2003

Episodic Tremor and Slip on the Cascadia Subduction Zone: The Chatter of Silent Slip

Garry Rogers* and Herb Dragert

We found that repeated slow slip events observed on the deeper interface of the northern Cascadia subduction zone, which were at first thought to be silent, have unique nonearthquake seismic signatures. Tremorlike seismic signals were found to correlate temporally and spatially with slip events identified from crustal motion data spanning the past 6 years. During the period between slips, tremor activity is minor or nonexistent. We call this associated tremor and slip phenomenon episodic tremor and slip (ETS) and propose that ETS activity can be used as a real-time indicator of stress loading of the Cascadia megathrust earthquake zone.

The Cascadia subduction zone is a region that has repeatedly ruptured in great thrust earthquakes of moment magnitude greater than 8 (*1*, *2*). Recently, slip events have been detected on the deeper (25- to 45-km) part of the northern Cascadia subduction zone interface by observation of transient surface deformation on a network of continuously recording Global Positioning System (GPS) sites (*3*). The slip events occur down-dip from the currently locked, seismogenic portion of the subduction zone (*4*), and, for the geographic region around Victoria, British Columbia, (Fig. 1), repeat at 13- to 16-month intervals (*5*). These slips were not accompanied by earthquakes and were thought to be seismically silent. However, unique nonearthquake signals that accompany the occurrence of slip have been identified using data from the regional digital seismic network. These pulsating, tremorlike seismic signals are similar to those reported in the forearc region of Japan (*6*, *7*), but the signals observed in Cascadia correlate temporally and spatially with six deep slip events that have occurred over the past 7 years. At other times, this tremor activity is minor or nonexistent. These tremors have a lower frequency content than nearby earthquakes, and they are uncorrelated with the deep or shallow earthquake patterns in the region. They have been observed only in the subduction zone region and specifically in the same region as the deep slip events. We refer to this associated tremor and slip phenomenon as episodic tremor and slip (ETS).

The seismic tremors described here are different from small earthquakes. The frequency content is mainly between 1 and 5 Hz, whereas most of the energy in small earthquakes is above 10 Hz. A tremor onset is usually emergent and the signal consists of pulses of energy, often about a minute in duration. A continuous signal may last from a few minutes to several days. Tremors are strongest on horizontal seismographs and move across the seismic network at shear wave velocities. A tremor on an individual seismograph is unremarkable and does not appear different from transient noise due to wind or cultural sources. It is only when a number of seismograph signals are viewed together that the similarity in the envelope of the seismic signal at each site identifies the signal as ETS (Fig. 1).

The tremor activity migrates along the strike of the subduction zone in conjunction with the deep slip events at rates ranging from about 5 to 15 km per day. Sometimes there is a gradual migration, but at other times there is a sudden jump from one region of the subduction fault to another. Tremors vary in amplitude, and the strongest can be detected as far as 300 km from the source region. During an ETS event, tremor activity lasts about 10 to 20 days in any one region and contains tremor sequences with amplitudes that are at least a factor of 10 larger

Geological Survey of Canada, Pacific Geoscience Centre, 9860 West Saanich Road, Sidney, British Columbia, Canada V8L 4B2.

*To whom correspondence should be addressed. E-mail: rogers@pgc.nrcan.gc.ca

than the minimum detectable tremor amplitude. Because of the emergent nature of the tremors, they are difficult to locate as precisely as nearby earthquakes using standard earthquake location procedures. Arrival times of coherent bursts detected across the network suggest source depths of 20 to 40 km, with uncertainties of several kilometers. Deeper solutions are to the northeast, and all solutions are near or just above the subduction interface. The fact that surface displacement patterns have been satisfactorily modeled using simple dislocations of 2 to 4 cm on the plate interface bounded by the 25- and 45-km depth contours (*3*) strongly suggests a spatial correlation with the source region of tremors.

To establish the temporal correlation between the slip events and the tremor activity (Fig. 2), we established the timing of six slip events observed on southern Vancouver Island since 1997 by cross-correlating changes in the east-west component of the Victoria GPS site (ALBH) with a symmetric 180-day sawtooth function, which replicated an average slip time series (*8*). This approach allowed the resolution of the midpoint of the slips to within 2 days. The duration of the slips, estimated from slope breaks in the ALBH time series, varied from 6 to 20 days. Seismic data were then examined at corresponding times to check for tremor activity. In each case, it was observed that sustained tremor activity on southern Vancouver Island coincided with the occurrence of slip (Fig. 2). For five of the slip events, tremors continued to migrate north along the axis of Vancouver Island, moving beyond the region of diagnostic GPS coverage.

To test a one-to-one correspondence, we examined continuous digital seismic data from the beginning of 1999 to the end of the 2003 tremor event to look for tremor activity outside the time windows of the slip events. No substantial activity was found for southern Vancouver Island, although a few periods with scattered low-amplitude tremor activity were observed in most months. Sustained large-amplitude tremor events have also been observed in northern and mid-Vancouver Island, as continuations of tremors migrating from the south and as independent tremor events. This implies that the ETS process occurs over the full length of the northern Cascadia subduction zone, but GPS coverage at the northern end is sparse, and surface displacements indicative of slip at depth have not been identified.

The cause of the tremor is not clear. Obara (*6*) has suggested fluids as a source for similar tremors in Japan. Because the tremor observed in Cascadia is mainly composed of shear waves, and because it correlates with slip that is relieving stress due to convergence (*3*), a shearing source seems most likely. However, because of the abundance of available fluids from the subducting plate in the subduction forearc (*9*), fluids may play an important role in the ETS process by regulating the shear strength of rock.

If the one-to-one correlation between transient slip and seismic signatures proves to be robust, then the tremorlike seismic signals can provide a real-time indicator of the occurrence of slip. Because slip events on the deep slab interface increase the stress across the locked plate interface located up-dip, it is conceivable that a slip event could trigger a large subduction thrust earthquake (*10*, *11*). Consequently, the onset of ETS activity could lead to recognized times of higher probability for the occurrence of megathrust earthquakes in the Cascadia subduction zone.

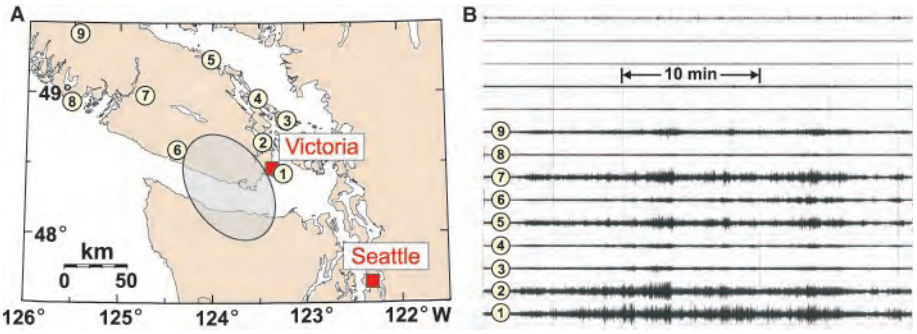

Fig. 1. (**A**) Map of seismic network sites (numbered circles) and approximate source region (shaded ellipse) for tremors used for correlation with observed slips. It has been observed that tremors and slip migrate parallel to the strike of the subduction zone to the north and south, as well as through this shaded region. (**B**) Sample seismic records of tremor activity at selected sites. It is the similarity of the envelope of the seismic signal on many seismographs that identifies ETS activity.

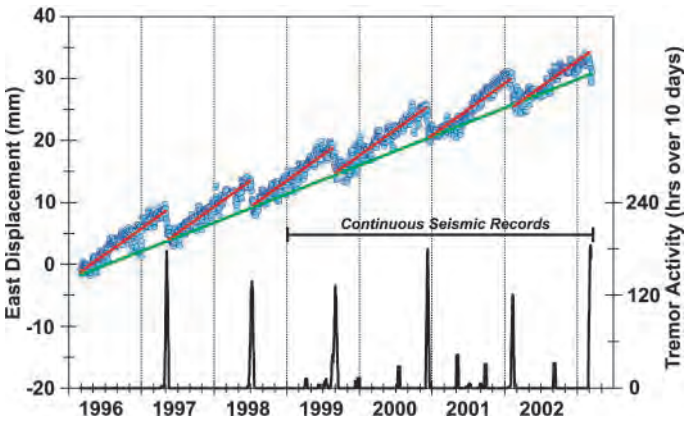

Fig. 2. Comparison of slip and tremor activity observed for the Victoria area. Blue circles show day-by-day changes in the east component of the GPS site ALBH (Victoria) with respect to the GPS site near Penticton, which is assumed to be fixed on the North America plate. The continuous green line shows the long-term (interseismic) eastward motion of the site. Red line segments show the mean elevated eastward trends between the slip events, which are marked by the reversals of motion every 13 to 16 months. The bottom graph shows the total number of hours of tremor activity observed for southern Vancouver Island within a sliding 10-day period (continuous seismic data were examined from 1999 onward). Ten days corresponds to the nominal duration of a slip event. The graph ends 10 March 2003, with the slip and tremor activity that was predicted for the spring of 2003.

References and Notes

1. B. F. Atwater *et al*., *Earthquake Spectra* **11**, 1 (1996).
2. K. Satake, K. Shimazake, Y Tsuji, K. Ueda, *Nature* **378**, 246 (1996).
3. H. Dragert, K. Wang, T. S. James, *Science* **292**, 1525 (2001).
4. H. Dragert, R. D. Hyndman, G. C. Rogers, K. Wang, *Geophys. Res*. **99**, 653 (1994).
5. M. M. Miller *et al*., *Science* **295**, 2423 (2002).
6. K. Obara, *Science* **296**, 1679 (2002).
7. A. Katsumata, N. Kamaya, *Geophys. Res. Lett*. **30**, 1020 (2003).
8. Precise dates for slip events were derived as follows: First, linear regression was used to estimate the long-term linear trend of the observed time series, corrected for offsets introduced by GPS antenna changes. Next, approximate dates (to within a week) for slip transients were identified from a visual inspection of the time series, and regression was again used to estimate an annual signal, the magnitude of the offsets at the time of the slips, and the average linear trend for the time periods between slip events. A 180-point symmetric sawtooth time series was generated using the average interslip trend and the average value of the offsets. This abbreviated sawtooth function was cross-correlated with the original observed (but de-trended) time series and the maxima for the cross-correlation function were used to establish the midpoint of slip events.
9. S. M. Peacock, *Science* **248**, 329 (1990).
10. W. Thatcher, *Nature* **299**, 12 (1982).
11. A. T. Linde, P. G. Silver, *Geophys. Res. Lett*. **16**, 1305 (1989).

12. We thank M. Schmidt and Y. Lu for their support in GPS network operations; R. Baldwin, T. Claydon, and R. Hall for their support in seismic network operations; and J. Cassidy and W. Bentkowski for help in locating tremors. This paper is Geological Survey of Canada contribution no. 2003022.

21 March 2003; accepted 29 April 2003
Published online 8 May 2003;
10.1126/science.1084783
Include this information when citing this paper.